Struct Multidisc Optim (2007) 34:261–275
DOI 10.1007/s00158-006-0072-4

MEDICAL AND BIOENGINEERING APPLICATIONS

Three-dimensional shape optimization of hip prostheses using a multicriteria formulation

Rui B. Ruben · João Folgado · Paulo R. Fernandes

Received: 4 July 2006 / Revised: 4 October 2006 / Published online: 4 January 2007

Abstract A multicriteria optimization model is developed to obtain the optimal geometry of the femoral component of a hip prosthesis. The objective function minimizes both the relative tangential displacement and the contact normal stress. For cementless stems, these two factors are relevant for the prosthesis stability and therefore for the implant success. The three-dimensional optimization procedure developed allows us to characterize the stem shape that minimizes displacement and stress individually, or simultaneously using a multicriteria approach. Design variables characterize successive stem sections, and are subjected to linear geometric constraints to obtain clinically admissible geometries. Multiple loads are considered to incorporate several daily life activities. The system bone–stem is considered a structure in equilibrium with contact condition on the interface. Results show that thin stem tips minimize the interface stress while collared stems minimize displacement. The multicriteria formulation leads to balanced solutions.

Keywords Shape optimization · Multicriteria optimization · Biomechanics · Hip prosthesis · Stem stability · Contact analysis

R. B. Ruben
School of Technology and Management,
Polytechnic Institute of Leiria,
Leiria, Portugal
e-mail: rbruben@estg.ipleiria.pt

R. B. Ruben · J. Folgado · P. R. Fernandes (✉)
IDMEC, IST,
Av. Rovisco Pais,
Lisbon 1049-001, Portugal
e-mail: prfernan@dem.ist.utl.pt

J. Folgado
e-mail: jfolgado@dem.ist.utl.pt

1 Introduction

Computational mechanics tools, including optimization procedures, were intensively applied to study biomechanical problems. One can find examples of this application on bone mechanics, where bone remodeling models were developed based on optimality criteria (see, e.g., Fernandes et al. 1999), and in prosthesis design (see, e.g., Huiskes and Boeklagen 1989; Fernandes et al. 2004). These powerful tools are very attractive to analyze and design medical devices and, in this paper, they are applied to design the femoral component of a hip prosthesis.

A total hip arthroplasty is the replacement of the natural joint by an artificial one, to relieve pain caused by trauma or joint disease. It involves the replacement of both the acetabular and femoral sides. On the femoral side a stem is placed into the marrow cavity, while on the acetabular side a cup is attached to pelvic bone (see Fig. 1). These prostheses can be classified as cemented or cementless devices. Cemented prostheses are fixed by polymethylmethacrylate (bone cement) while the fixation of cementless prostheses is obtained by biological fixation. The cementless stem is directly applied into a canal made by the surgeon and stem and bone should fit adequately to minimize interfacial micromotion and allow bone ingrowth (osseointegration). A porous coating is usually applied on stem surface to promote osseointegration. For cementless stems with porous coating the initial fixation is purely mechanical and an adequate initial fixation is determinant for biological fixation along the prosthesis lifetime. Actually, long-term success of cementless hip prosthesis is strongly related with initial stability of the femoral stem, i.e., "small" relative displacements between bone and stem and "small" contact stresses, promote bone ingrowth into the prosthesis porous coating, essential for biologic fixation.

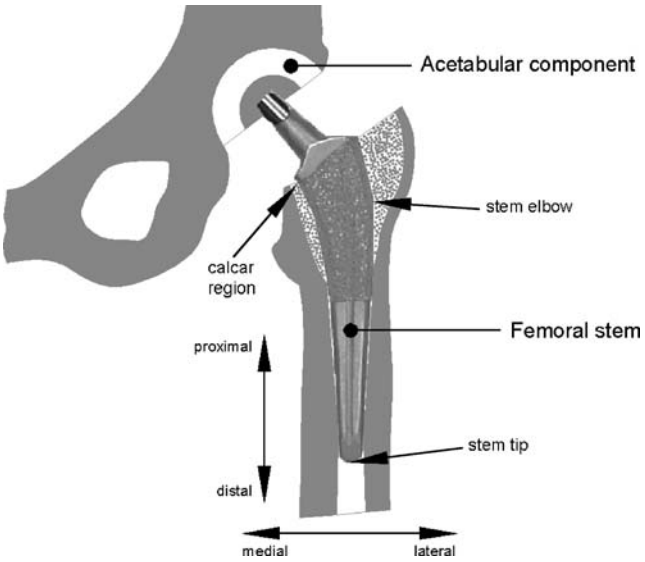

Fig. 1 Total hip replacement

Furthermore, "large" relative displacements and "large" contact stresses can originate thigh pain (see, e.g., Herzwurm et al. 1997). The initial stability is therefore related with the most important cause of cementless stem failure, the aseptic loosening resulting from an inefficient fixation between bone and stem. This inefficient fixation is often related with the formation of a layer of soft tissue (Viceconti et al. 2001). This layer of soft tissue can also be induced by debris from joint contact friction. In fact, inflammatory reactions and osteolysis (loss of bone tissue by gradual disintegration), with larger incidence in unstable stems, are generally caused by wear particles (Huo et al. 1995). In addition, after a total hip arthroplasty, bone tissue starts an adaptive process because the bone mechanical environment is changed. Long-term bone remodeling is very important for prosthesis success and it also depends on initial conditions, such as primary stability and host-bone quality (Fernandes et al. 2002; García et al. 2002).

The two mechanical parameters determinant for initial stability are interface displacement and contact stresses. The threshold of interface displacement value to have bone ingrowth is not precisely known. For instance, Rancourt et al. (1990) refers 28 μm as limit value for the displacement to have bone ingrowth while for Viceconti et al. (2001) limit values are between 30 and 150 μm and displacements between 150 and 220 μm lead to the formation of a fibrous layer, preventing complete fixation. With respect to contact stresses, cortical bone has ultimate compression strength of 170 MPa and ultimate tensile strength of 124 MPa (Fung 1993).

A question is how the stem design can influence the initial stem stability and prostheses success. Actually, the relation between cementless hip arthroplasty success and initial stability depends on different factors: biologic response to metallic stem, surgery technique, friction, host-bone quality, and stem geometry (Bernakiewicz et al. 1999; Huo et al. 1995). For instance, noncircular sections do not need surgical cylindrical reamers. In this way, trabecular bone and blood supply are preserved to achieve bone ingrowth rapidly (Swanson 2005). From a biomechanical point of view, stem geometry and porous coating length can be studied to improve initial stability and, therefore, also improve implant durability. However, stem shape is constrained by anatomic factors, and thus some restrictions to three-dimensional model of prosthesis should be considered.

To address the problem of the relation between geometry (stem design) and prosthesis performance, some shape optimization models were developed. Yoon et al. (1989) defined the stem shape, minimizing the stress concentration in the cement. In the same year, Huiskes and Boeklagen (1989) presented a model to optimize the shape of a cemented stem with the objective of minimizing the stress in the cement. This work was part of a research program with surgeons and bioengineers to obtain a new cemented stem, which culminated with the scientific hip prostheses (Biomet Europe). Katoozian and Davy (2000) developed a model to optimize cemented and cementless stems, minimizing three different objective functions. The first two are stress functions applied either to cement or surrounding bone, the third one is a function of bone and cement strain energy density. Bonded interfaces were considered for cemented and uncemented prostheses, and optimized shapes are all large in the proximal part (part closer to the femur head). Kowalczyk (2001) presented an optimization procedure to minimize the stress on bone–stem interface of cementless stems. Kowalczyk also considered bonded interface in coated regions and contact without friction in uncoated zones. In his work the design variables define only the stem axial lengths.

In Fernandes et al. (2004), a two-dimensional optimization model to obtain the shape of a hip stem to minimize the relative displacement and normal stress on bone–stem interface was presented. In the present work this model is extended to the three-dimensional case. Therefore, a multicriteria optimization procedure is developed to obtain the three-dimensional stem shape with better initial stability. The optimization model uses a multicriteria formulation that permits simultaneous minimization of relative tangential displacement and contact stress on bone–stem interface. Design variables are 17 geometric parameters describing successive stem sections. These parameters are subjected to geometric constraints to obtain clinically admissible shapes. The state variables, i.e., the relative displacement and contact stress, are the solution of the equilibrium problem with contact conditions between femur and stem. This equilibrium problem is solved by the finite element method. The contact formulation allows the analysis of different

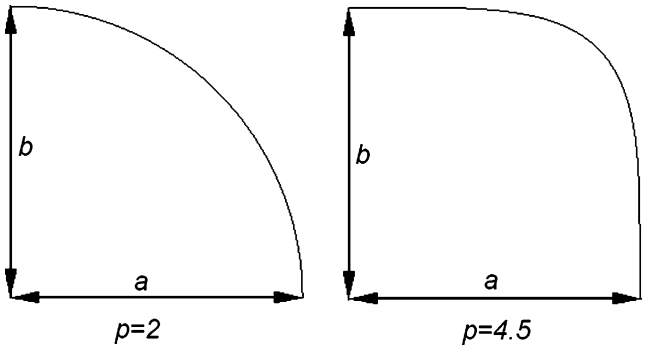

Fig. 2 Influence of parameter p in (1), representation of first quadrant, $a=b$

porous coating lengths and, for this purpose, it was considered two different lengths: totally coated and half-coated stems. A multiple load formulation, with three load cases, was also used to simulate different daily life activities. The optimization problem was solved numerically by a hybrid method combining the method of moving asymptotes (MMA) (Svanberg 1987) and the gradient projection method. The objective functions gradients were computed using forward finite differences. The three-dimensional stem geometries obtained lead to a better understanding of the relation between stem design, coating length, and initial stem stability.

The results of this work are in accordance with other scientific works and some features of the obtained optimal shapes are already present in commercial hip stems. For instance, the effect of the collar on displacement is in agreement with the study of Keaveny and Bartel (1993), and stem tips are often slender to avoid direct contact with cortical bone (see, e.g., Romagnoli 2002).

2 The shape optimization model

A multicriteria shape optimization model is developed to simultaneously minimize the relative displacement and the contact stress on bone–stem interface. This optimization process was applied to a three-dimensional model of the femoral component (stem) of a total hip arthroplasty. In this section the initial geometry and the respective design variables are defined and the finite element model is presented. Then the formulation of the optimization problem is stated as well as the strategy to solve it numerically.

2.1 Design variables and initial geometry

To define the design variables let us consider the stem transversal sections defined by:

$$\left(\frac{x}{a}\right)^p + \left(\frac{y}{b}\right)^p = 1 \tag{1}$$

in a local system xy. The parameters a, b, and p characterize the section shape as shown in Fig. 2. With $a=b$ the section

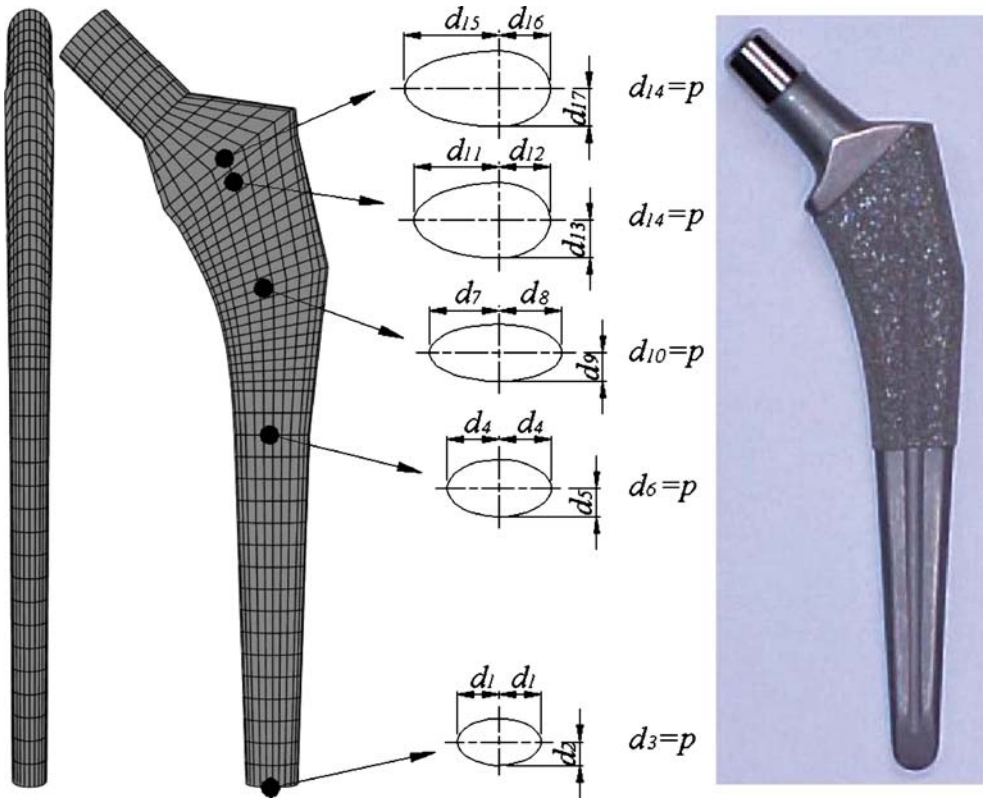

Fig. 3 Initial geometry, design variables (section dimensions are not scaled), and the Tri-Lock stem

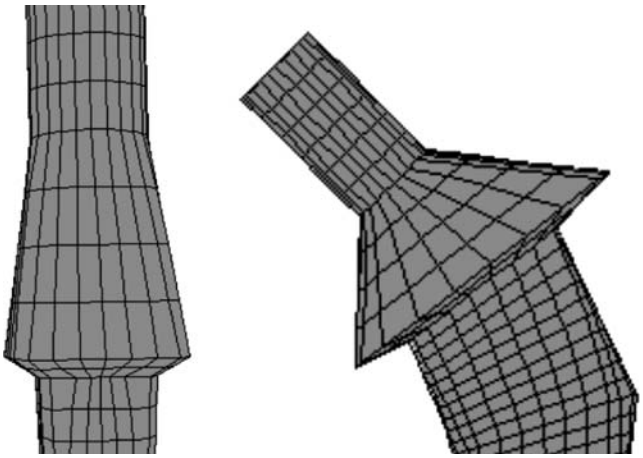

Fig. 4 Example of a collar

is circular for $p=2$ and goes to a square when p increases. For $a \neq b$ circular and squared sections became elliptic and rectangular, respectively. The 17 design variables ($\boldsymbol{d}$) define the five key sections presented in Fig. 3. These design variables correspond to parameters a, b, and p defined in (1). A suitable interpolation of the key sections is used to obtain the entire three-dimensional geometry. It should be noted that a B-spline was used to interpolate the points generated by d_4, d_7, and d_{11}. The initial geometry was based on the commercial Tri-Lock prosthesis from DePuy (see Fig. 3).

With the parameterization defined above it is possible to obtain a collar. The potential collar is defined by variables d_{15}, d_{16}, and d_{17}, which define the section above the bone edge, and by d_{11}, d_{12}, and d_{13} from the upper section inside the femur (see Fig. 4). The collar can avoid stem over-insertion and subsidence (sliding into the femur). However, there are some criticisms of collared designs because it can compromise the distal fit (Mandell et al. 2004). With the present multicriteria model, collared and collarless optimized stem shapes can be obtained and its advantages and disadvantages can be discussed.

For every 17 design variables upper and lower bounds are defined to maintain the stem inside the bone. In addition, ten linear constraints are considered to obtain clinically admissible stem shapes.

$$
\begin{aligned}
&h_1 = d_1 - d_4 \leq 0; \quad h_2 = d_2 - d_5 \leq 0; \quad h_3 = d_4 - d_7 + c_3 \leq 0; \quad h_4 = d_4 - d_8 \leq 0;\\
&h_5 = d_5 - d_9 \leq 0; \quad h_6 = d_7 - d_{11} + c_6 \leq 0; \quad h_7 = d_{12} - d_8 \leq 0; \quad h_8 = d_9 - d_{13} \leq 0;\\
&h_9 = d_{11} - d_7 + c_9 \leq 0; \quad h_{10} = d_7 - \frac{d_{11} + d_4}{2} \leq 0
\end{aligned}
\tag{2}
$$

Constraints h_3, h_6, and h_9 are defined to obtain splines with negative slope tangent lines, as illustrated in Fig. 5a,b, and constraint h_{10} assures a convex spline, as illustrated in Fig. 5c. The values for c_3, c_6, and c_9 depends on geometry and in this case they are $c_3=c_6=3.5$ and $c_9=-9$.

It should be noted that these constraints are introduced to ensure that it is possible to insert the stem inside the bone, maintaining the contact between the stem and the biological tissues, i.e., to obtain feasible prosthesis. Without these constraints, the optimization process can lead to shapes

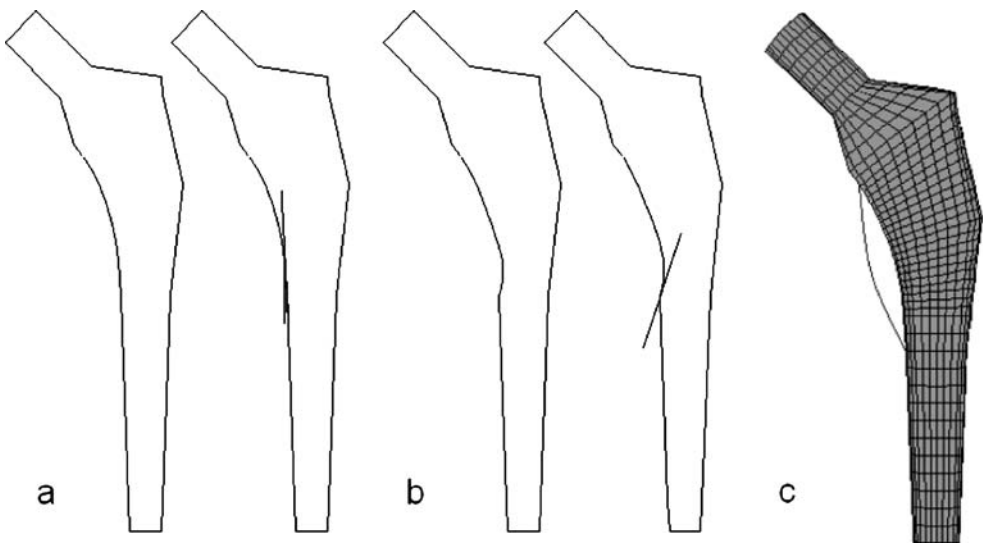

Fig. 5 **a** Tangent with negative slope, **b** tangent with positive slope, and **c** convex and concave spline

Table 1 Load intensities

		F_x (N)	F_y (N)	F_z (N)
Load case 1	F_h	224	972	−2,246
	F_a	−768	−726	1,210
Load case 2	F_h	−136	630	−1,692
	F_a	−166	−382	957
Load case 3	F_h	−457	796	−1,707
	F_a	−383	−669	547

x medial-lateral, y anterior-posterior, z distal-proximal

that, at least, imply special insertion techniques or difficult the removal process, as reported in Huiskes and Boeklagen (1989).

2.2 Load cases

Three load cases were considered to simulate different daily life activities (Kuiper 1993). The problem was first solved for the single load case situation, applying each load case individually, and then for a multiple load case considering the effect of successive loads. In Table 1 and Fig. 6, load intensities and directions are presented.

2.3 The problem formulation

The main goal of this shape optimization problem is to obtain a hip prosthesis with better primary stability. To improve the stability for cementless stems it is essential to reduce the relative tangential displacement and contact stresses. For these conditions, the optimization problem can be stated as:

$$\begin{aligned} &\min_{d_i} f(\boldsymbol{d}) \\ &\text{such that } (l_i)_{\min} \le d_i \le (l_i)_{\max} \qquad i = 1, 2, \ldots, 17 \\ &\qquad h_j(\boldsymbol{d}) \le 0 \qquad j = 1, 2, \ldots, 10 \end{aligned} \tag{3}$$

where $(l_i)_{\min}$ and $(l_i)_{\max}$ are the lower and upper bounds of design variables d_i, and h_j is the set of constraints defined by (2) to ensure admissible clinically shapes. For the objective function $f(\boldsymbol{d})$ three hypothesis were considered:

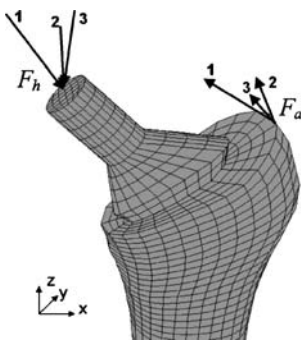

Fig. 6 Load cases

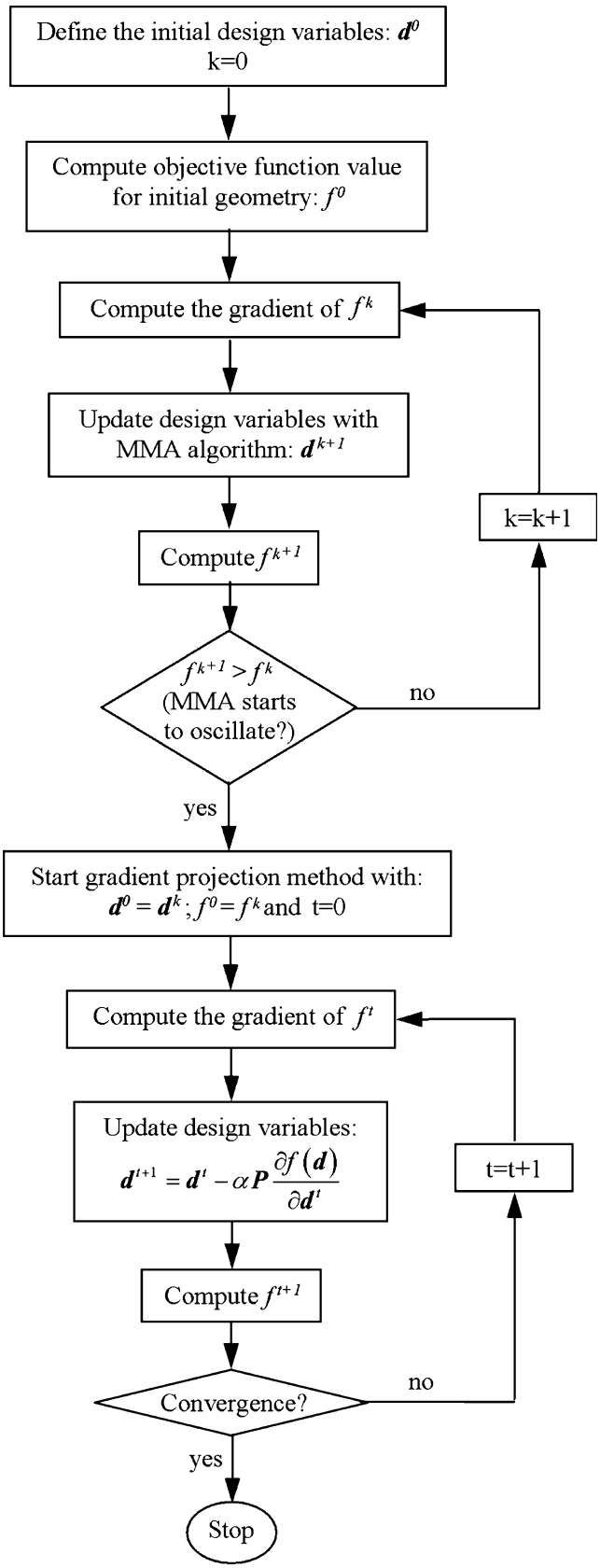

Fig. 7 Optimization procedure flowchart

Table 2 Sensitivity derivatives for several differential quotients δ, objective function f_d, half-coated stem, load case 3, and initial geometry

d_i	δ					
	Backward		Forward			
	0.0001	0.00001	0.00001	0.0001	0.001	0.01
d_1	−0.6823	−0.6820	−0.6819	−0.6816	−0.6784	−0.6462
d_2	11.7231	11.7239	11.7241	11.7248	11.7326	11.8105
d_3	11.6457	11.6456	11.6456	11.6456	11.6451	11.6464
d_4	−12.2007	−12.2006	−12.2005	−12.2004	−12.1990	−12.1847
d_5	2.5767	2.5773	2.5774	2.5780	2.5837	2.6403
d_6	−2.7139	−2.7133	−2.7132	−2.7127	−2.7071	−2.6523
d_7	6.1339	6.1340	6.1340	6.1341	6.1349	−3.7145
d_8	−4.2869	−4.2868	−4.2868	−4.2868	−4.2865	−4.2837
d_9	4.7705	4.7708	4.7708	4.7711	4.7739	4.8020
d_{10}	2.6830	2.6830	2.6830	2.6830	2.6833	−7.1160
d_{11}	−8.8485	−8.8486	−8.8485	−8.8483	−8.8475	−8.8388
d_{12}	1.9099	1.9099	1.9099	1.9099	1.9099	1.9105
d_{13}	0.9828	0.9828	0.9828	0.9828	0.9828	0.9834
d_{14}	−3.0136	−3.0144	−3.0146	−3.0153	−3.0228	−3.0970
d_{15}	−0.3138	−0.3138	−0.3138	−0.3138	−0.3137	−0.3135
d_{16}	−0.2026	−0.2026	−0.2026	−0.2026	−0.2027	−0.2028
d_{17}	−1.0549	−1.0549	−1.0549	−1.0548	−1.0548	−1.0542

Table 3 Sensitivity derivatives for several differential quotients δ, objective function f_t, half-coated stem, load case 3, and initial geometry

d_i	δ					
	Backward		Forward			
	0.0001	0.00001	0.00001	0.0001	0.001	0.01
d_1	19.9625	19.9627	19.9628	19.9630	19.9650	19.9849
d_2	3.1956	3.1955	3.1955	3.1954	3.1945	3.1849
d_3	4.9389	4.9385	4.9384	4.9380	4.9339	4.9071
d_4	0.5036	0.5037	0.5037	0.5039	0.5051	0.5180
d_5	7.0974	7.0976	7.0977	7.0979	7.1000	7.1216
d_6	2.6904	2.6906	2.6906	2.6907	2.6922	2.7067
d_7	−4.0297	−4.0296	−4.0296	−4.0296	−4.0294	−0.6134
d_8	−2.4383	−2.4383	−2.4383	−2.4383	−2.4382	−2.4369
d_9	−4.5567	−4.5566	−4.5566	−4.5565	−4.5553	−4.5433
d_{10}	−7.7163	−7.7159	−7.7159	−7.7155	−7.7119	−4.2567
d_{11}	−0.9468	−0.9469	−0.9468	−0.9468	−0.9469	−0.9481
d_{12}	−0.3890	−0.3890	−0.3890	−0.3890	−0.3890	−0.3889
d_{13}	−5.4937	−5.4937	−5.4937	−5.4935	−5.4927	−5.4837
d_{14}	−10.0463	−10.0463	−10.0463	−10.0463	−10.0463	−10.0458
d_{15}	0.0161	0.0161	0.0161	0.0161	0.0161	0.0161
d_{16}	0.0093	0.0093	0.0093	0.0093	0.0093	0.0093
d_{17}	0.2008	0.2008	0.2008	0.2008	0.2008	0.2008

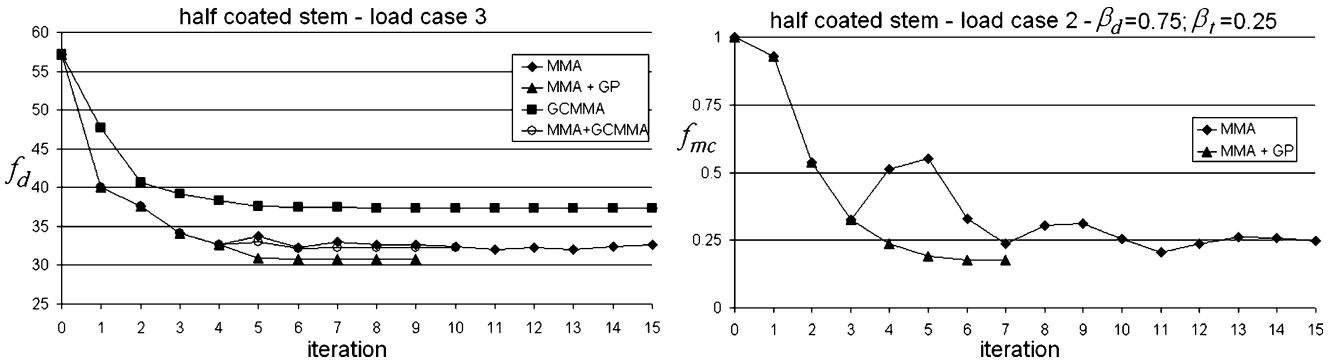

Fig. 8 Convergence analysis for several tested methods (MMA, MMA + GP, GCMMA, and MMA + GCMMA) for half-coated stem, objective functions f_d and f_{mc}

a function of tangential interfacial displacement,

$$f_d = \sum_{P=1}^{NC} \left(\alpha_P \frac{10^5}{\Gamma_c} \int_{\Gamma_c} \left| \left(u_t^{rel}\right)_P \right|^2 d\Gamma \right) \tag{4}$$

or a function of normal contact stresses,

$$f_t = \sum_{P=1}^{NC} \left(\alpha_P \frac{1}{\Gamma_c} \int_{\Gamma_c} \left| (\tau_n)_P \right|^2 d\Gamma \right) \tag{5}$$

or, finally, a multicriteria function combining the previous ones,

$$f_{mc} = \beta_d \frac{f_d - f_d^0}{f_d^i - f_d^0} + \beta_t \frac{f_t - f_t^0}{f_t^i - f_t^0} \tag{6}$$

This multicriteria function is defined based on a weighting objective method as described in Osyczka (1992).

In (4) and (5) NC is the number of applied loads, α_P are the load weight factors, with $\sum_{P=1}^{NC} \alpha_P = 1$, $\left(u_t^{rel}\right)_P$ and $(\tau^n)_P$ are the relative tangential displacement and the normal stress on bone–stem contact surface Γ_c, for load case P. In (6) f_d^0 and f_t^0 are the minimums of f_d and f_t, respectively; f_d^i and f_t^i are the initial values of f_d and f_t, respectively; and β_d and β_t are the weighting coefficients with $\beta_d + \beta_t = 1$.

The relative displacement $\left(u_t^{rel}\right)_P$ and the contact stress $(\tau_n)_P$, for each load case P, are the solution of the equilibrium problem with contact conditions.

2.4 Computational model

2.4.1 Optimization algorithm

Computationally, the optimization problem is solved after the flowchart shown in Fig. 7. First, for a given set of initial variables $\boldsymbol{d}$, the objective function (f_d, f_t, or f_{mc}) is computed using the values of interface displacement and contact stress, which is the solution of the contact problem solved with the finite element program ABAQUS (ABAQUS 2003).

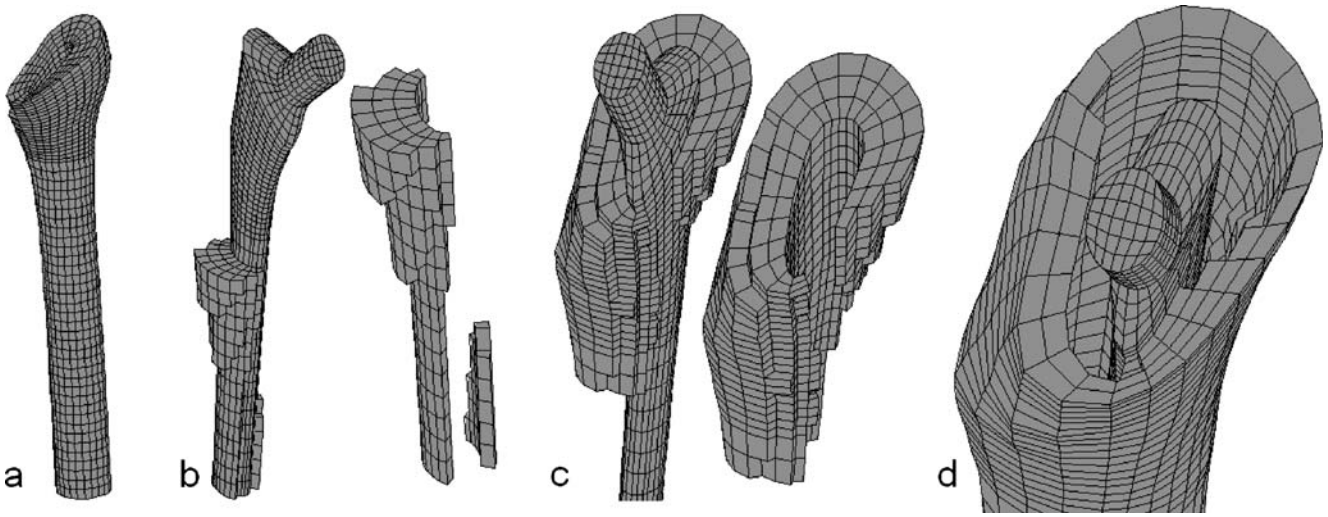

Fig. 9 **a** Femur, **b** stem and marrow, **c** stem and trabecular bone, and **d** stem and cortical bone

Table 4 Material properties

	E (GPa)	ν
Cortical bone	17	0.3
Trabecular bone	1	0.3
Bone marrow	10^{-7}	0.3
Stem	115	0.3

Table 5 Objective function values: minimization of f_d

	Coating length	f_d initial	f_d final
Load case 1	Totally coated	51.54	28.79
	Half-coated	72.69	34.74
Load case 2	Totally coated	29.17	14.95
	Half-coated	35.74	17.48
Load case 3	Totally coated	48.79	24.39
	Half-coated	57.14	30.77
Multiple load case	Totally coated	43.17	23.02
	Half-coated	55.19	27.52

With the contact formulation, it is possible to analyze different porous coating lengths. In the present work two coating lengths were considered, a totally coated stem and a half-coated stem (similar to the Tri-Lock stem shown in Fig. 3). Coated and uncoated surfaces are modeled as contact surfaces with and without friction, respectively. The friction coefficient is assumed to be equal to 0.6.

Once the objective function is computed, the sensitivity derivatives are obtained using forward finite differences. The sensitivity derivatives for both single objective functions are summarized in Tables 2 and 3. These results stand for initial geometry, half-coated stem and load case 3. It must be noticed that, for both objective functions and for all the design variables tested, a good convergence is achieved (as the interval δ goes to zero). This behavior is also verified for the other load cases and coating extent.

After the gradient computation, the optimization method starts. At the initial stage of the development of this research, a simple gradient projection method (see, e.g., Luenberger 1989) was used, however, a very slow convergence was experienced. For this reason, the MMA (Svanberg 1987) was tested because it is characterized by a fast convergence. Actually, MMA is based on a convex approach for the objective function and this monotonous approach gives to MMA the fast convergence property. However, MMA is not a globally convergent method (Svanberg 1995) and there are examples where oscillations are noticed near the optimal solution (Zuo et al. 2005; Bruyneel et al. 2002). In the present optimization problem, MMA also oscillates near the optimal solution. Thus, an optimization scheme that combines the MMA with a gradient projection method is proposed. Firstly, MMA is used to approach the solution to the optimal point and then the gradient projection method starts to avoid numerical oscillations. This approach corresponds to a hybrid optimization method also proposed by other authors with MMA-based methods (Zuo et al. 2005; Bruyneel et al. 2002).

A preliminary analysis was performed to compare the performance of several optimization methods: the MMA method, a globally convergent MMA (GCMMA) presented in Svanberg (1995), a hybrid method combining MMA and GCMMA (MMA + GCMMA), and the hybrid method used in this paper, MMA combined with a gradient projection method (MMA + GP). The analysis is graphically presented in Fig. 8.

The fast convergence and the oscillations of the MMA method was observed. Using the MMA followed by the gradient projection method showed to be a good strategy to solve this particular problem of stem shape optimization.

2.4.2 Finite element model

The optimization algorithm described above is applied to a suitable finite element discretization. To obtain such a model it is necessary to have an accurate geometry of the femur and femoral stem. The finite element model was

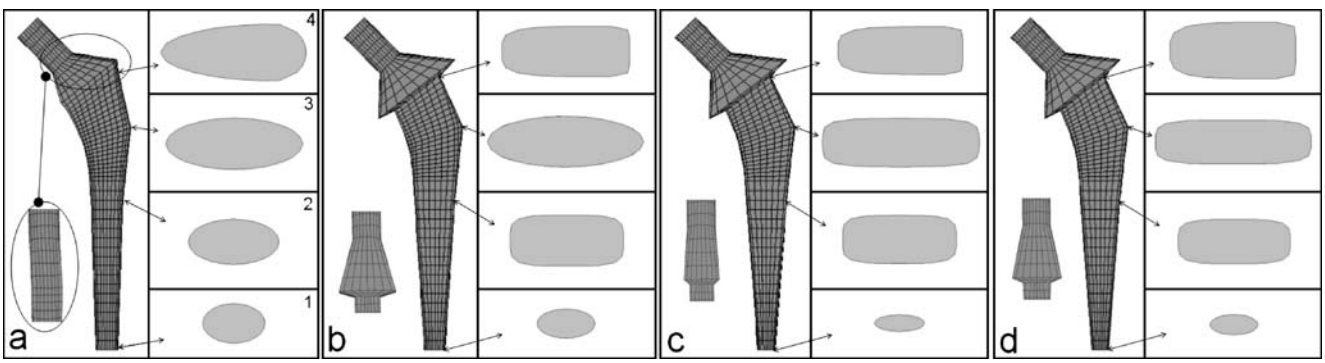

Fig. 10 **a** Initial geometry. Optimized geometries, totally coated stems, function f_d; **b** load case 1, **c** load case 3, and **d** multiple load case

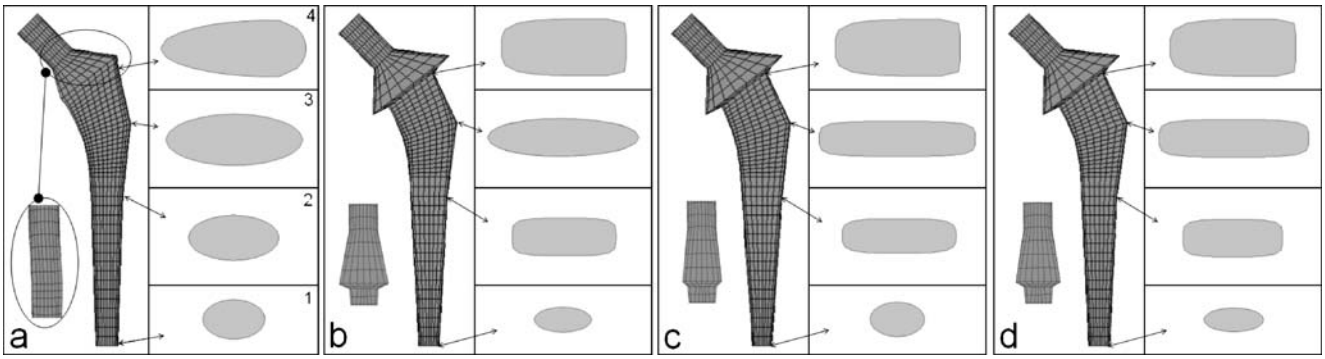

Fig. 11 **a** Initial geometry. Optimized geometries, half-coated stems, function f_d; **b** Load case 2, **c** load case 3, and **d** multiple load case

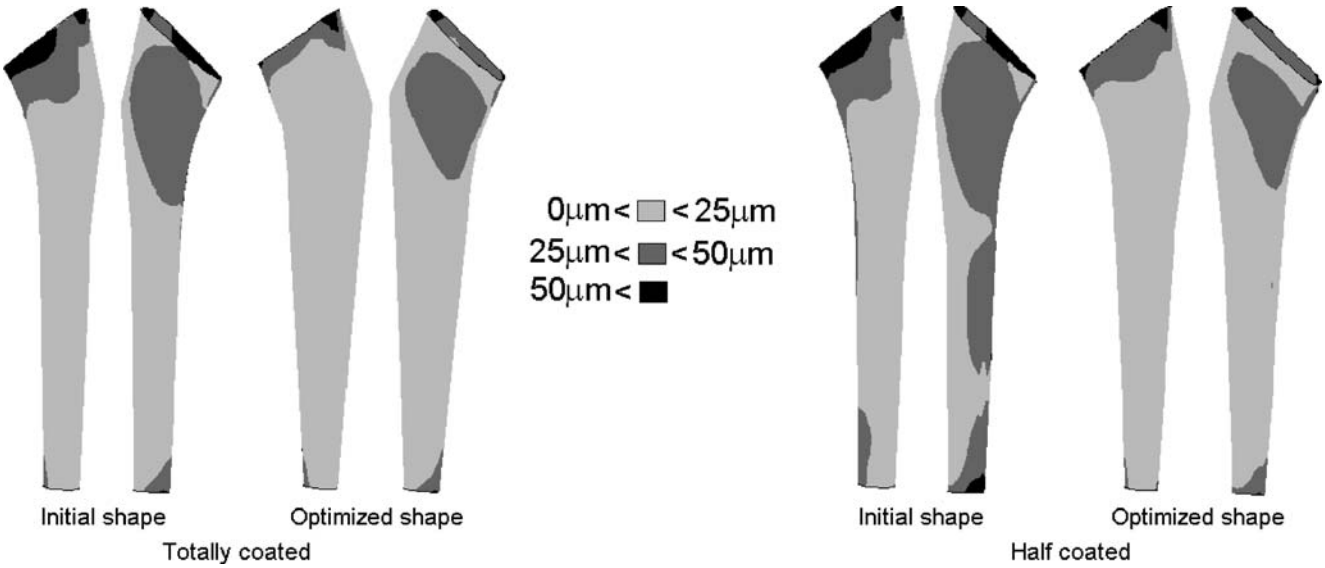

Fig. 12 Relative tangential displacement for the minimization of objective function f_d. Load case 1

build using a geometry based on the "standardized femur" (Viceconti et al. 1996). Because the femur is nonhomogeneous, the model considers marrow, cortical, and trabecular bone regions, as shown in Fig. 9. Within each region, properties of biologic tissues are assumed isotropic. With respect to the femoral stem, the initial geometry is based on the Tri-Lock stem from DePuy and the selected material is titanium (Ti-6Al-4V). Material properties for bone and stem are presented in Table 4.

The finite element mesh discretization has 7,176 eight-node solid elements, 1,800 elements for the stem, and 5,376 elements for the femur.

3 Results

3.1 Minimization of relative displacement: f_d

The problem was first solved for every single load and then for a multiple load case. Numerical results for the minimization of relative tangential displacement are presented in Table 5. For multiple load case, equal weight factors were considered: $\alpha_1=\alpha_2=\alpha_3=1/3$. Initial objective functions values for half-coated stems are greater than for totally coated ones. For optimized stems, totally coated prosthesis also presents lower values. In Figs. 10 and 11, it

Table 6 Objective function values: minimization of f_t

	Coating length	f_t initial	f_t final
Load case 1	Totally coated	30.00	10.81
	Half-coated	48.59	11.09
Load case 2	Totally coated	16.82	5.17
	Half-coated	24.42	5.53
Load case 3	Totally coated	30.29	9.48
	Half-coated	48.51	10.43
Multiple load case	Totally coated	25.70	8.43
	Half-coated	40.51	10.00

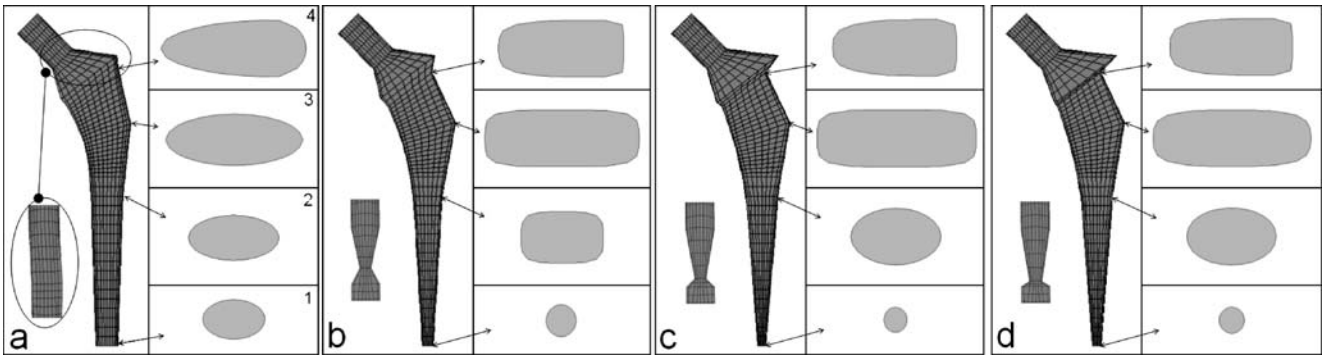

Fig. 13 **a** Initial geometry. Optimized geometries, totally coated stems, function f_t; **b** load case 1, **c** load case 3, and **d** multiple load case

is possible to compare the initial shape with optimized ones for totally coated and half-coated stems, respectively.

All optimized shapes, in Figs. 10 and 11, present a collar to avoid subsidence, i.e., sliding inside the femur. Section 2 (see section numbers in Figs. 10a or 11a) is larger (parameter a) and more rectangular (parameter p) than the initial one, improving the fixation on cortical bone. Section 3 is larger for optimized shapes to improve the contact between compact bone and the stem elbow (see Fig. 1). Rectangular sections 3 and 4 are also important to reduce torsion and bending effects.

For all load cases, sections 1 and 2 define a distal wedge shape, which is slightly fixed on cortical bone diminishing the displacement. Indeed, there are similarities on optimal shape for the different load cases, thus, the multiple load solution reflects this fact.

In Fig. 12 it is possible to observe that the area with displacements below 25 μm increases from initial to optimized shapes. Furthermore, for optimized shapes, displacements greater than 50 μm are concentrated in small portions of proximal and distal regions, and they are always smaller than 100 μm. This means that even assuming bone ingrowth is inhibited for displacement above 25 μm, which is a conservative value, large porous coated regions will be candidate to an efficient biological fixation.

3.2 Minimization of contact stress: f_t

In Table 6 numerical results for contact stress objective function are summarized. Values of the objective function for totally coated stems are lower than those obtained for half-coated prosthesis. In Figs. 13 and 14 it is possible to compare the initial shape with optimized ones. For the multiple load case, weight factors are assumed equal to one third.

Usually, the maximum normal contact stress is observed at the stem tip (see Fig. 1). To minimize the stress objective function, it is necessary to reduce this peak stress. For this purpose, a small circular stem tip (section 1) is the ideal shape because it stays surrounded by marrow and never directly touches the cortical bone.

In Figs. 13 and 14, it is possible to observe that sections 2, 3, and 4 are thicker (parameter b) than the initial solution to increase the contact surface and thus to minimize stress in medial side, particularly in the calcar region.

In some cases a small lateral collar appears in the optimal solution. The stresses in this lateral side slightly increase, but it leads to a stress reduction on the calcar region (medial side). However, the overall contribution of this effect in the reduction of the stress objective function is small when compared with the contribution achieved in the distal region of the stem.

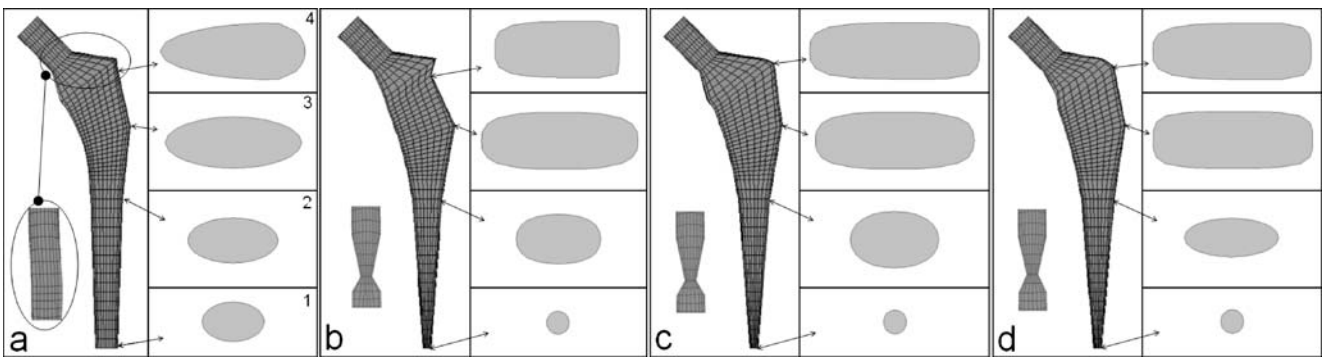

Fig. 14 **a** Initial geometry. Optimized geometries, half-coated stems, function f_t; **b** load case 1, **c** load case 2, and **d** multiple load case

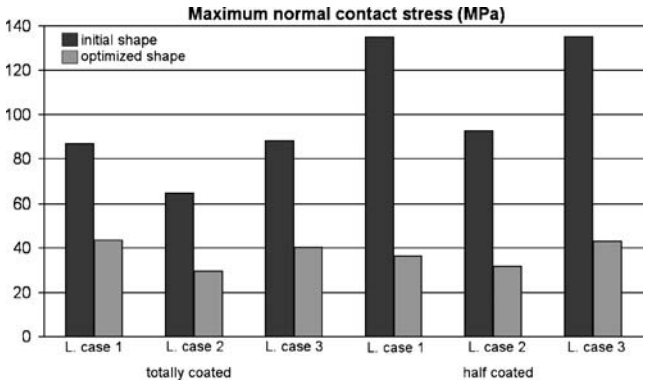

Fig. 15 Maximum contact stress for the minimization of objective function f_t

When the objective function for contact stress is minimized the maximum contact stress is significantly reduced, as observed in Fig. 15. For optimized geometries all stress values are below 45 MPa and far from the ultimate strength for cortical bone: 170 MPa in compression and 124 MPa in tension (Fung 1993).

3.3 Multicriteria optimization: f_{mc}

Some optimized shape characteristics obtained for displacement objective function are opposite to those obtained for stress objective function. However, to improve initial stability it is necessary to reduce tangential relative displacement and contact normal stress. Therefore, a multicriteria formulation allows us to simultaneously minimize both single objectives.

With a multicriteria optimization algorithm it is possible to obtain a set of nondominated points. In Table 7 nondominated points are presented for three coefficient pairs of (6), (β_d, β_t)=(0.25, 0.75), (0.5, 0.5), and (0.75, 0.25), and also for single objective optimization, i.e., (β_d, β_t)=(0, 1) and (1, 0).

Figures 16 and 17 show the shapes obtained with the multicriteria optimization and multiple load formulation for totally coated and partially coated stems, respectively. In these figures, the nondominated points are also graphically depicted together with the single objective points. The solution for (β_d, β_t)=(0.75, 0.25) have a bigger collar to minimize the displacement objective function. In addition, point (β_d, β_t)=(0.75, 0.25) presents the larger section 1 (parameter a) to fix the stem on cortical bone. Small distal section avoids direct contact between the stem tip and the cortical bone, which is suitable to minimize stresses. Also, the thickest section 3 (parameter b) is observed for (β_d, β_t)=(0.25, 0.75) to minimize stress.

Compared with the initial geometry, all nondominated points have larger regions with tangential relative displacement below 25 μm. Regions with tangential displacement below 25 μm also increase from point (β_d, β_t)=(0.25, 0.75) to point (β_d, β_t)=(1, 0). For all multicriteria optimized shapes, only very small proximal and distal areas have tangential relative displacement greater than 50 μm (Figs. 18 and 19).

In Figs. 20 and 21, the normal contact stress distribution for some nondominated points is shown. In both figures, it is clear that the peak of stress is in the stem tip, and only the point (β_d, β_t)=(0.75, 0.25), where the weight of the stress function is lower than the displacement function, has a considerable region with stress greater than 50 MPa. When the weight for the stress function increases the region with high stress is reduced, showing the importance of considering the multicriteria formulation.

3.4 Discussion of the results

The major features of the optimal shapes obtained in this work are in accordance with other scientific works and they are already present in commercial hip stems.

Concerning the beneficial influence of the collar in the reduction of the displacement, this was already reported by other investigators such as Keaveny and Bartel (1993). The collar is also present in some commercial models such as Bi-Metric with collar from Biomet Europe. However, there

Table 7 Objective function values: minimization of f_{mc}

	Coating length	(β_d, β_t)=(0, 1)		(β_d, β_t)=(0.25, 0.75)		(β_d, β_t)=(0.5, 0.5)		(β_d, β_t)=(0.75, 0.25)		(β_d, β_t)=(1, 0)	
		f_d	f_t	f_d	f_t	f_d	f_t	f_d	f_t	f_d	f_t
Load case 1	Totally coated	78.99	10.81	37.70	12.51	32.03	14.94	30.58	16.75	28.79	25.99
	Half-coated	132.38	11.09	50.20	15.32	41.80	20.24	36.37	26.53	34.74	38.32
Load case 2	Totally coated	41.20	5.17	19.47	6.55	16.93	7.92	16.09	9.23	14.95	13.20
	Half-coated	69.92	5.53	28.45	7.04	19.92	11.34	19.01	13.99	17.48	21.02
Load case 3	Totally coated	64.84	9.48	29.94	11.51	28.24	12.81	25.16	16.37	24.39	21.72
	Half-coated	106.34	10.43	40.31	12.71	36.70	15.53	31.10	23.31	30.77	37.22
Multiple load case	Totally coated	72.49	8.43	30.44	9.91	25.83	12.36	23.70	14.99	23.02	17.25
	Half-coated	75.08	10.00	40.68	11.23	31.75	16.29	30.06	25.42	27.52	35.68

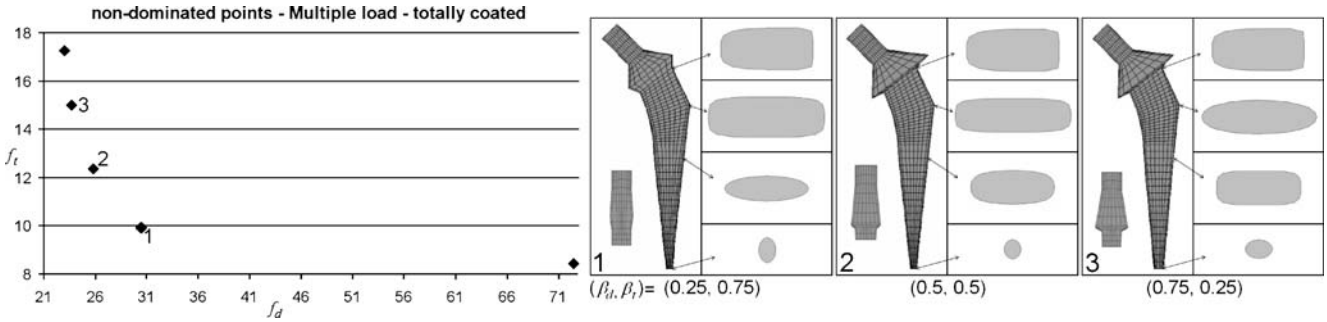

Fig. 16 Nondominated points. Objective function f_{mc}. Multiple load case. Totally coated

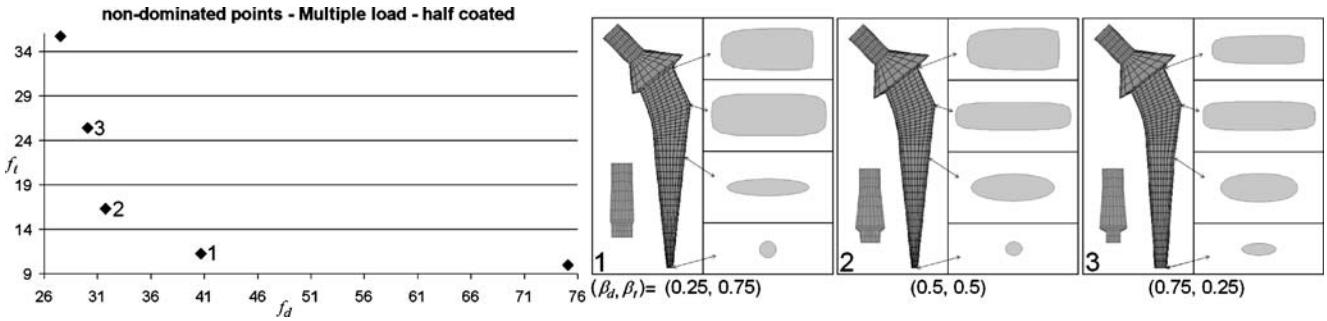

Fig. 17 Nondominated points. Objective function f_{mc}. Multiple load case. Half-coated

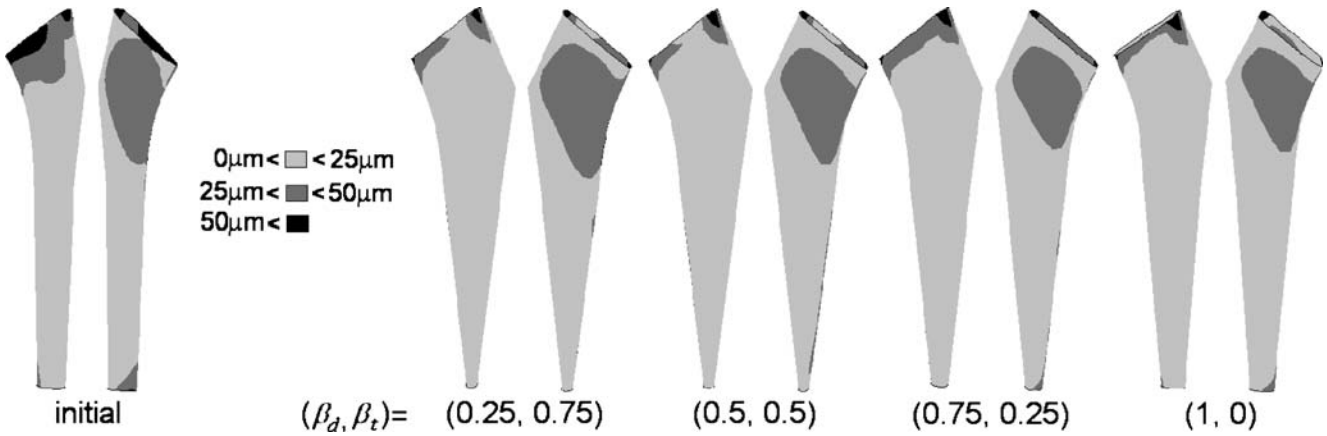

Fig. 18 Relative tangential displacement due to load case 1. Minimization of objective function f_{mc}, multiple load case, and totally coated stem

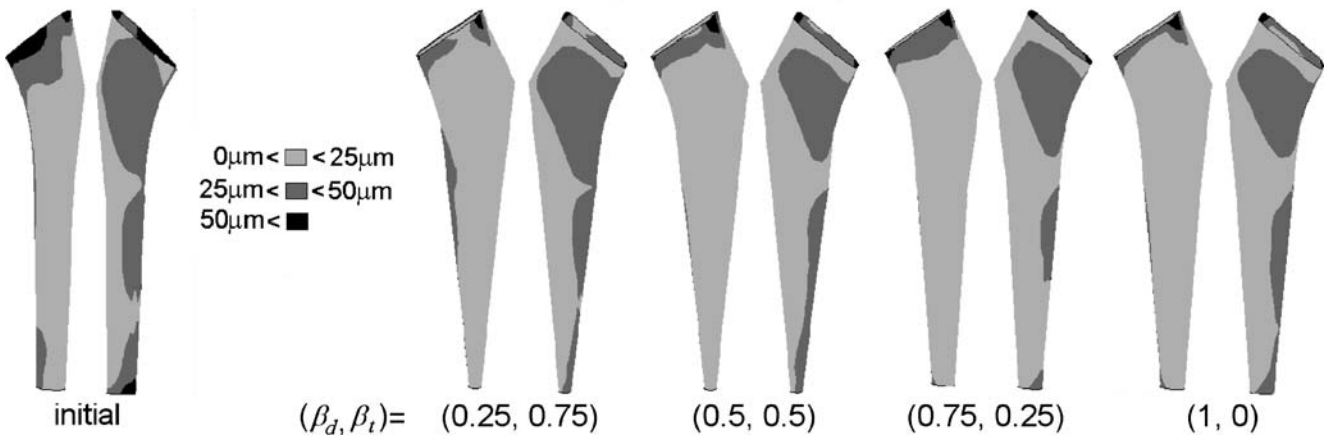

Fig. 19 Relative tangential displacement due to load case 1. Minimization of objective function f_{mc}, multiple load case, and half-coated stem

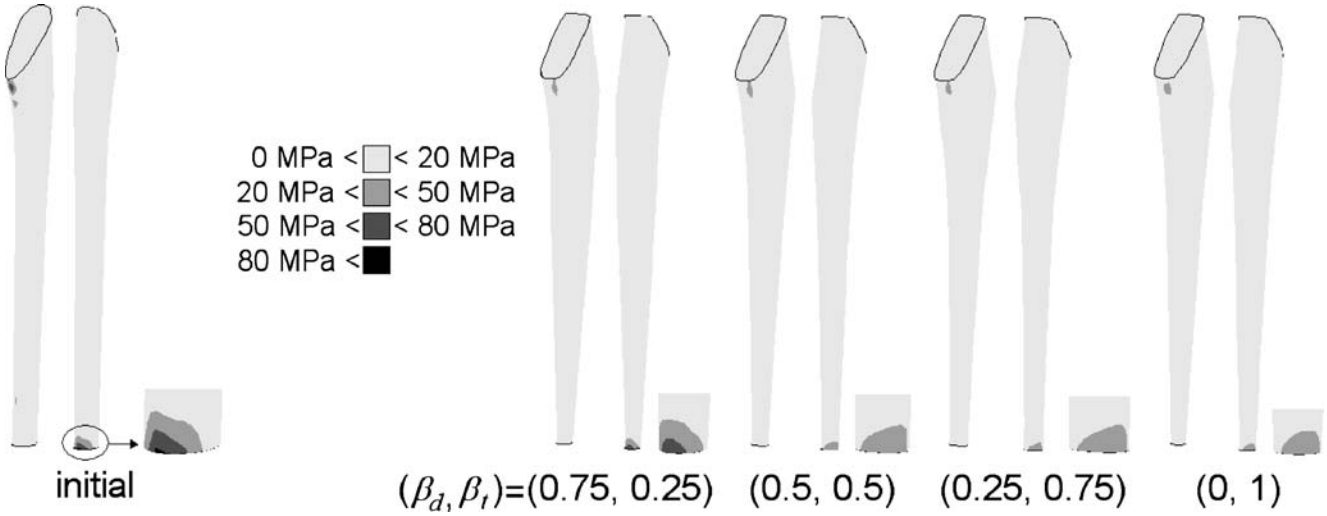

Fig. 20 Normal contact stress due to load case 3. Minimization of objective function f_{mc}, multiple load case, and totally coated stem

are some negative opinions about the presence of the collar in the hip stem (Mandell et al. 2004). One point is that bone necrosis is sometimes found in the calcar region bellow the collar, and if bone damage takes place, the collar support is lost. Another argument is the difficulty of conveniently inserting a collared stem to simultaneously obtain a good collar support and a good adjustment between bone and stem in the intramedullary canal.

With respect to the stem tip, several studies have noticed that there is a high stress concentration in the surrounding bone. Furthermore, the contact peak stress on stem tip is often related with thigh pain and can originate a revision surgery. To diminish this peak stress, several design solutions were proposed. One of the solutions is to thin the stem tip to avoid direct contact with cortical bone, as in the cementless Spotorno stem from Sulzer Orthopedics (Romagnoli 2002). This type of geometry for the distal part of the stem also reduces the bending stiffness. In fact, reducing the distal stiffness is a way to diminish the peak stress. In their work, Dorr and Wan (1996) established a clinical correlation between the distal stiffness and the thigh pain. It should be noted that the stiffness reduction can be obtained actuating on shape and on the stem material.

Regarding the cross-section, some authors claim for rectangular shapes to have a better rotational stability than circular ones (see, e.g., Huo et al. 1995). The obtained optimal shapes with respect to displacement objective function have sections number 2 almost rectangular, as can be observed in Zweymuller stem design. These totally coated prosthesis have rectangular sections and wedge design to offer excellent rotational and axial stability. For this prosthesis only 3 months after surgery new trabecular bone formation on bone–stem interface is observed and 5 years later almost 100% of patients have no pain and have good stem stability (Huo et al. 1995; Swanson 2005).

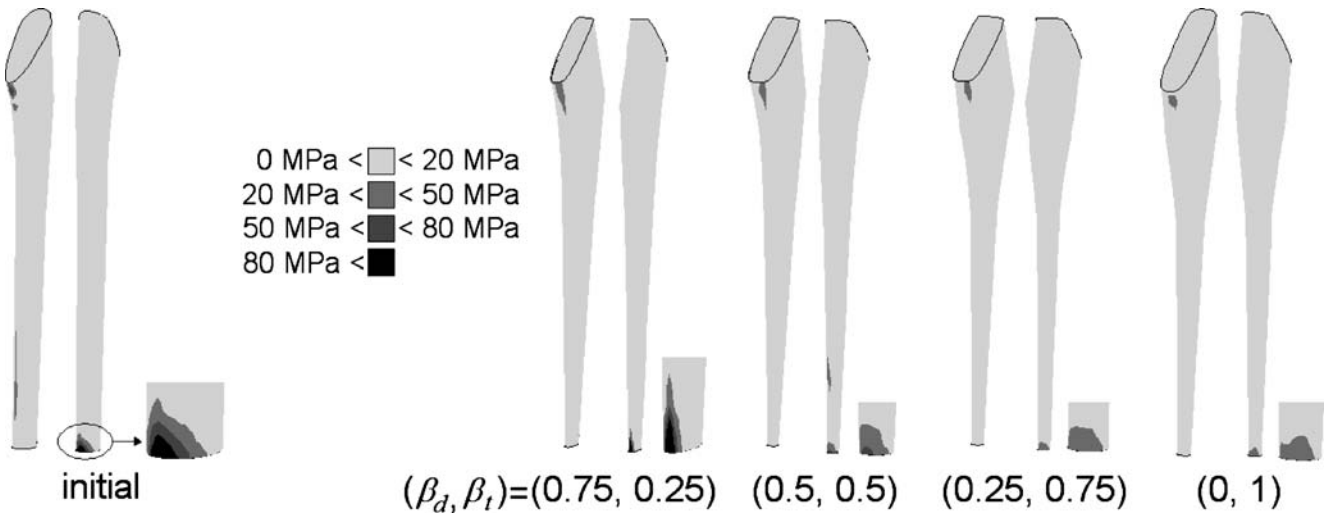

Fig. 21 Normal contact stress due to load case 3. Minimization of objective function f_{mc}, multiple load case, and half-coated stem

4 Final remarks

A three-dimensional shape optimization model to obtain cementless hip stem geometries was presented. The main goal was the minimization of relative tangential displacement and normal contact stress, using a single and a multicriteria objective function. A multiple load formulation was also considered to incorporate different daily life activities. The bone–stem set is considered a structure in equilibrium with contact conditions.

The two single objective functions results are contradictory. The minimization of displacement leads to stems with a collar and a wedge design for the distal stem with a stem tip large enough to fix on cortical bone. These features avoid stem subsidence. The minimization of contact stress leads to thin distal tips, marrow surrounded, without touching cortical bone directly. It was demonstrated that the multicriteria algorithm developed in this work is very efficient to deal with these two contradictory objectives. From a computational point of view the obtained optimized shapes are better than the initial ones, i.e., the initial stability was considerably improved. The displacement obtained for optimized shapes are within the range of biological values that permits bone ingrowth. In addition, for contact stress objective function the peak of stress obtained is under the strength limit for bone. Results fairly agree with some tendencies in commercial femoral components and with other scientific and clinical works, as shown in the previous section.

It should be noticed that in this study all optimization processes considered a healthy femur. Nevertheless, different clinical situations can be considered in the present model. For instance, bones with osteoporosis can originate a more difficult initial stability and a fast adverse remodeling process. Also, different initial conditions can be studied, such as different contact conditions on interface, and their influence on primary stability can be investigated. Another factor that changes the mechanical bone strength and leads to prosthesis failure is the stress-shielding effect and the consequent bone remodeling. To incorporate this factor, an extension of this shape optimization process including bone remodeling is being developed.

Notwithstanding continuing efforts to refine the method, this model leads to useful conclusions on the relation between shape, porous coating, and stem stability. This information is important for new prosthesis design and for surgeons who have to decide among numerous commercial stem shapes.

References

ABAQUS (2003) ABAQUS, version 6.4. HKS, RI, USA

Bernakiewicz M, Viceconti M, Toni A (1999) Investigation of the influence of periprosthetic fibrous tissue on the primary stability of uncemented hip prostheses. In: Middleton J, Jones ML, Shrive NG, Pande GN (eds) Computer methods in biomechanics & biomedical engineering—3. Gordon and Breach, NY, USA, pp 21–26

Bruyneel M, Duysinx P, Fleury C (2002) A family of MMA approximations for structural optimization. Struct Multidiscipl Optim 24:263–276

Dorr LD, Wan Z (1996) Comparative results of a distal modular sleeve, circumferential coating, and stiffness relief using the anatomic porous replacement II. J Arthroplast 11(4):419–428

Fernandes PR, Rodrigues H, Jacobs C (1999) A model of bone adaptation using a global optimization criterion based on the trajectorial theory of Wolff. Comput Methods Biomech Biomed Eng 2:125–138

Fernandes PR, Folgado J, Jacobs C, Pellegrini V (2002) A contact model with ingrowth control for bone remodelling around cementless stems. J Biomech 35:167–176

Fernandes PR, Folgado J, Ruben RB (2004) Shape optimization of a cementless hip stem for a minimum of interface stress and displacement. Comput Methods Biomech Biomed Eng 7(1):51–61

Fung YC (1993) Biomechanics: mechanical properties of living tissues, 2nd edn. Springer, Berlin Heidelberg New York

García JM, Doblaré M, Cegoñino J (2002) Bone remodelling simulation: a tool for implant design. Comput Mater Sci 25:110–114

Herzwurm PJ, Simpson S, Duffin S, Oswald SG, Ebert FR (1997) Thigh pain and total hip arthroplasty. Clin Orthop Relat Res 336:156–161

Huiskes R, Boeklagen R (1989) Mathematical shape optimization of hip prosthesis design. J Biomech 22:793–804

Huo MH, Martin RP, Zatorski LE, Keggi KJ (1995) Total hip arthroplasty using Zweymuller stem implant without cement. J Arthroplast 10(6):793–799

Katoozian H, Davy DT (2000) Effects of loading conditions and objective function on three-dimensional shape optimization of femoral components of hip endoprostheses. Med Eng Phys 22:243–251

Keaveny T, Bartel D (1993) Effects of porous coating, with and without collar support, on early relative motion for a cementless hip prosthesis. J Biomech 26(12):1355–1368

Kowalczyk P (2001) Design optimization of cementless femoral hip prostheses using finite element analysis. J Biomech Eng 123:396–402

Kuiper JH (1993) Numerical optimization of artificial joint designs. Ph.D. thesis, Katholieke Universiteit Nijmegen

Luenberger DG (1989) Linear and nonlinear programming, 2nd edn. Addison-Wesley, Reading, MA

Mandell JA, Carter DR, Goodman SB, Shurman DJ, Beaupré GS (2004) A conical-collared intramedullary stem can improve stress transfer and limit micromotion. Clin Biomech 19:695–703

Osyczka A (1992) Computer aided multicriterion optimization system (CAMOS) software package in Fortran. International Software Publishers, Cracow, Poland

Rancourt D, Shirazi-Adl A, Drouin G, Paiment G (1990) Friction properties of interface between porous-surfaced metals and tibial cancellous bone. J Biomed Materi Res 24:1503–1519

Romagnoli S (2002) Press-fit hip arthroplasty, a European alternative. J Arthroplast 17(4 Suppl 1):108–112

Svanberg K (1987) The method of moving asymptotes—a new method for structural optimization. Int J Numer Methods Eng 24:359–373

Svanberg K (1995) A globally convergent version of MMA without linesearch. In: Olhoff N, Rozvany GIN (eds) First world congress of structural and multidisciplinary optimization. Pergamon, Oxford, pp 9–16

Swanson TV (2005) The tapered press fit total hip arthroplasty. J Arthroplast 20(4 Suppl 2):63–67

Viceconti M, Casali M, Massari B, Cristofolini L, Bassani S, Toni A (1996) The 'standardized femur program' proposal for a

reference geometry to be used for the creation of finite element methods of the femur. J Biomech 29:1241

Viceconti M, Monti L, Muccini R, Bernakiewicz M, Toni A (2001) Even a thin layer of soft tissue may compromise the primary stability of cementless hip stems. Clin Biomech 16: 765–775

Yoon YS, Jang GH, Kim YY (1989) Shape optimal design of the stem of a cemented hip prosthesis to minimize stress concentration in the cement layer. J Biomech 22:1279–1284

Zuo KT, Chen LP, Zhang YQ, Yang J (2005) A hybrid topology optimization algorithm for structural design. Eng Optim 37(8): 849–866